LETTER

Anomalous oscillatory features in neutron emission from D + D fusion in palladium at 100 keV implantation energy

To cite this article: R. K. Choudhury *et al* 2019 *EPL* **126** 12002

A Letters Journal Exploring the Frontiers of Physics

April 2019

EPL, **126** (2019) 12002
doi: 10.1209/0295-5075/126/12002

www.epljournal.org

Anomalous oscillatory features in neutron emission from D + D fusion in palladium at 100 keV implantation energy

R. K. Choudhury, Ajay Kumar, R. G. Thomas[a], G. Mishra, A. Mitra, B. K. Nayak and A. Saxena

Nuclear Physics Division, Bhabha Atomic Research Centre - Mumbai - 400 085, India

received 22 November 2018; accepted in final form 16 April 2019
published online 22 May 2019

PACS 25.45.-z – Nuclear reactions: specific reactions: ^{2}H-induced reactions
PACS 26.20.-f – Nuclear astrophysics: Hydrostatic stellar nucleosynthesis
PACS 24.30.-v – Nuclear reactions: general: Resonance reactions

Abstract – Neutron yield in $D+D$ fusion in a palladium foil, kept at about $-76\,^{\circ}$C temperature, has been measured as a function of the number of implanted D^+ ions at a bombarding energy of 100 keV. A considerably large oscillatory pattern was observed riding on a systematic increment for the emitted neutron yield as a function of the number of implanted D^+ ions. Such an oscillatory behaviour is in contrast with the expected neutron yield calculated using the bare $D+D$ fusion cross-section. The present observation seems to indicate that the bare cross-section is significantly affected due to the lattice effects of the host metal at large D/Pd atomic ratios.

Introduction. – Nuclear fusion of light nuclei is of interest for both basic and applied nuclear physics. The $D+D$ and $D+T$ reactions are among the nuclear processes responsible for the production of light elements in nucleosynthesis [1,2]. These reactions are also very important for the development of neutron sources, fusion-fission hybrid systems and advancement of nuclear technologies for controlled fusion [2,3]. Though the bare $D+D$ reaction is well studied and established, large enhancements of the reaction yields observed for this nuclear reaction proceeding in a number of metallic host targets in several recent experiments have evoked considerable attention worldwide [4–10].

In general, the $D+D$ fusion follows two paths:

$$D+D \rightarrow T(1.01\,\mathrm{MeV}) + p(3.02\,\mathrm{MeV}), \quad (1)$$

$$\rightarrow {}^3\mathrm{He}(0.82\,\mathrm{MeV}) + n(2.45\,\mathrm{MeV}) \quad (2)$$

and the cross-section for the above reaction in the case of bare $D+D$ fusion at very low sub-barrier energies is written as

$$\sigma_b(E) = \frac{S(E)}{E}\exp(-2\pi\eta), \quad (3)$$

where $S(E)$ is the astrophysical S factor and η the Sommerfeld parameter. However, in the presence of Coulomb screening the above equation modifies to

$$\sigma_{scr}(E) = \frac{S(E)}{\sqrt{E(E+U_e)}}\exp\left[-\sqrt{\frac{E_G}{E+U_e}}\right], \quad (4)$$

where U_e is the screening potential and E_G is the Gamow energy, which is around 986 keV for the $D+D$ system [5]. This leads to an enhancement factor, $f(E)$, which is defined as

$$f(E) = \frac{\sigma_{scr}(E)}{\sigma_b(E)}. \quad (5)$$

Though the Coulomb barrier for pure $D+D$ fusion is ∼200 keV, detectable reaction rates may occur even at much lower kinetic energies ∼10–15 keV due to Coulomb screening [11–22]. Further, the dependence of the enhancement factor on the host material's temperature for the $D+D$ reaction is also an important topic being investigated recently [23–25].

In this work, we report the results of the experiments carried out to investigate the neutron yield in $D+D$ fusion during deuterium implantation in palladium at low temperatures. The paper is organized as follows: the experimental setup and the experimental procedure are described in the next section. In the following section, experimental results along with the simulations are discussed. The summary is given in the last section.

Experimental setup. – The experiments were performed using 100 keV D^+ ions provided by the Electron

[a]E-mail: rgthomas@barc.gov.in (corresponding author)

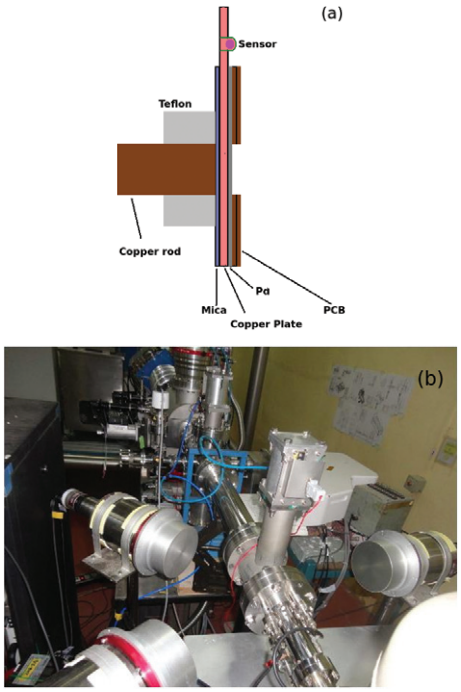

Fig. 1: (a) Schematic of the target assembly and (b) the photograph of the experimental setup.

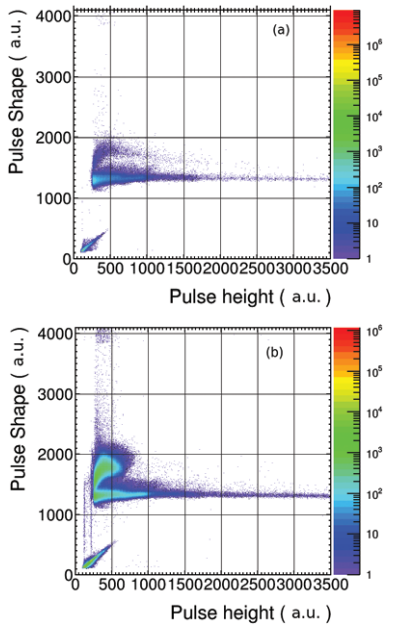

Fig. 2: 2D plots of pulse shape *vs.* pulse height for the ^{252}Cf source (a) and for the $D + D$ reaction (b).

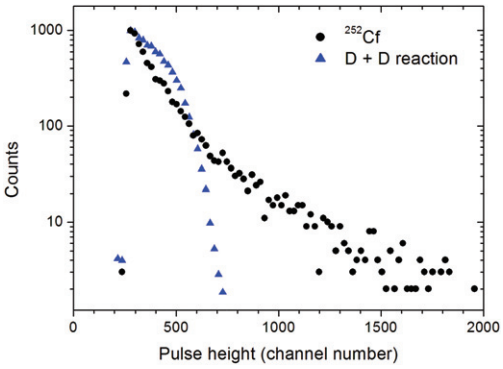

Fig. 3: Pulse height spectra of neutrons for the ^{252}Cf fission and $D + D$ fusion reactions.

Cyclotron Resonance (ECR) source at the Bhabha Atomic Research Centre, Mumbai. The accelerated D^+ ions impinged on a cooled palladium target. The target assembly (fig. 1) consisted of a solid copper rod (cold finger) of ∼25 cm length and diameter ∼2 cm with one end connected to a liquid-nitrogen cryocan. The other end of the cold finger was attached to a very thin copper disc through a thermoconducting electrically insulating paste. The palladium foil, which has a surface area ∼1.0 cm^2 (1.0 cm × 1.0 cm) and thickness of 2.5 μm was pasted onto the copper disc using a conducting silver paste. A resistance temperature detector (PT-100) was mounted on the copper disc to measure the temperature of the target region online. Provision was also made on the target to read the beam current. The entire target assembly was attached to the beam tube and was operated under high vacuum better than 1.0×10^{-6} mbar. The beam current was kept around 6–7 μA during the experiment. At equilibrium condition without the beam, the target temperature was −82.5 °C; however, the target temperature increased to −75.5 °C, −72 °C and −67.5 °C at 0.6 watt, 1 watt, 1.4 watt beam power, respectively. The average temperature of the Pd target was ∼−76 °C during the experiment as the current was maintained at about 6–7 μA.

The neutron detector setup consisted of three liquid scintillator detectors (each 127 mm × 50.8 mm) mounted at a distance of ∼30 cm from the target (fig. 1). Each of the neutron detectors was calibrated using the standard gamma sources of ^{137}Cs and ^{22}Na. The thresholds for all the three detectors were around 52.6 keV (D_1), 72.7 keV (D_2), and 70.6 keV (D_3) respectively. The intrinsic efficiency of the detectors D_1, D_2, and D_3 for 2.45 MeV neutrons was calculated to be around 42%, 40%, and 40%, respectively, using the GEANT4 [26] based Monte Carlo simulation for the corresponding threshold of a particular detector [27]. The pulse shape discrimination optimization was carried out using a ^{252}Cf source. A typical 2D graph of the same is shown in fig. 2(a). A typical 2D plot of pulse shape discrimination for the experimental $D+D$ reaction is shown in fig. 2(b). The pulse height spectra of neutrons corresponding to both the cases are given in fig. 3.

The neutron rates along with the incident ion beam current were monitored on-line as well as recorded in list mode using a VME-based DAQ system. All three neutron detector signals and the current integrator signal were used to create the logical OR condition to provide the master trigger for the acquisition system. The data were collected till the total number of implanted ions exceeded 3.5×10^{18}.

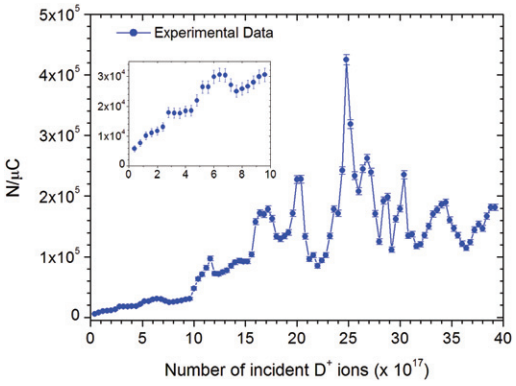

Fig. 4: Measured N/μC as a function of implanted D^+ ions. The inset shows a magnification of the region of implantation up to 7 $\times 10^{17}$ ions.

Data were collected also for the beam-off condition to monitor the ambiance background in the neutron region before and after the experiment.

Experimental results and simulations. – The neutron yield in each detector was corrected for the efficiency and the solid angle. Background correction for neutron counts was done corresponding to the duration of the beam-on time. Thereafter, the experimental data collected for all three detectors are summed for improved statistics and the results are shown in fig. 4 as neutrons per micro-Coulomb (N/μC) *vs.* the number of implanted D^+ ions. It was observed that the nature of the plot was found to be identical for all the three detectors. The inset in fig. 4 shows a magnified plot of the emitted neutron yield in the initial phase of implantation up to $\sim 10 \times 10^{17}$ D^+ ions. It is clearly seen from fig. 4 that N/μC shows a pronounced oscillatory pattern, riding on a systematic increment, as a function of the number of implanted D^+ ions. It should also be noted that the deviations observed are way beyond the statistical fluctuations, which are of the size of the symbol used. The amplitude of the oscillations keeps increasing and reaches a maximum at around $\sim 25 \times 10^{17}$ implanted D^+ ions, and then starts decreasing with a further increase in the number of implanted ions.

Simulations for the neutron yield as a function of the number of implanted ion were carried out using GEANT4 in combination with the EXFOR cross-section for $D + D$ fusion (bare) (fig. 5(a)). In general, the number of neutrons/s, N_n, from a thick target can be calculated using the following equation [28]:

$$N_n = N_d N_T \int_0^E \sigma_N(E) \left[\frac{\mathrm{d}E}{\mathrm{d}(\rho x)}\right]^{-1} \mathrm{d}E, \qquad (6)$$

where N_d is the number of incident particles/s, N_T is the number of target atoms/g, σ_N is the cross section for neutron production, $\frac{\mathrm{d}E}{\mathrm{d}(\rho x)}$ is the stopping power of the target material (keV/g/cm^2) and E is the incident energy. However, instead of using a continuous

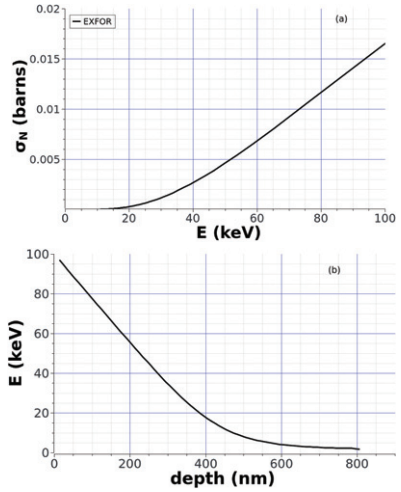

Fig. 5: (a) σ_N (EXFOR - $D(D,n)^3$He) used in the simulation and (b) the average energy of the beam as a function of depth.

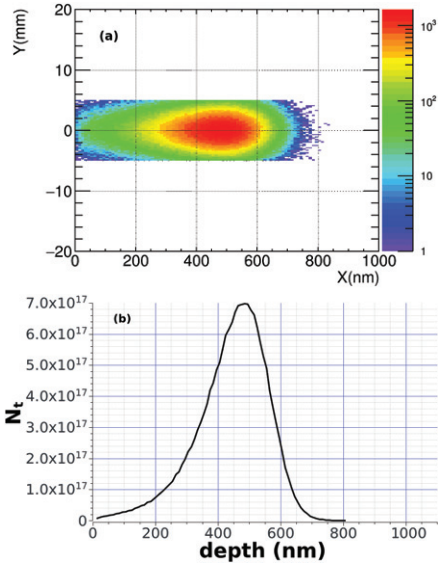

Fig. 6: (a) Two-dimensional density distribution of ions simulated using GEANT4 and (b) the number of ions per cm^2 (N_t) as a function of depth.

expression as defined above, we estimated the neutron yield by dividing the entire target thickness into 1 nm thick slices. The neutron yield from each slice was estimated as $n_i = N_d N_T \rho \mathrm{d}x \sigma_N(E_i)$, where E_i is the average energy (fig. 5(b)) of the deuterons in the i-th slice and dx is the thickness of each slice. Within a given slice, the energy E_i as well as the cross-section σ_N were kept constant. However, for the $(i+1)$-th slice, the energy of the deuteron beam is reduced by ΔE_i *i.e.*, the average energy loss in the i-th slice.

We have assumed that the implanted ions are localised and the diffusion is negligibly small owing to the low temperature preserving the initial ion distribution. The distribution of the implanted D^+ ions along the beam direction in the palladium foil was simulated using

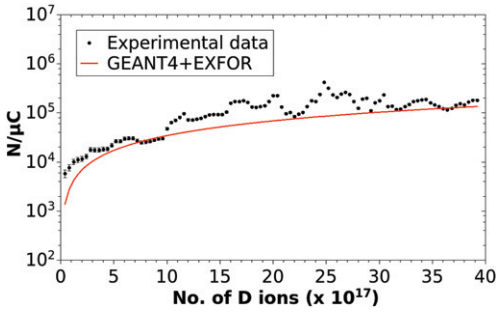

Fig. 7: The experimental and simulated value of N/μC as a function of implanted D^+ ions.

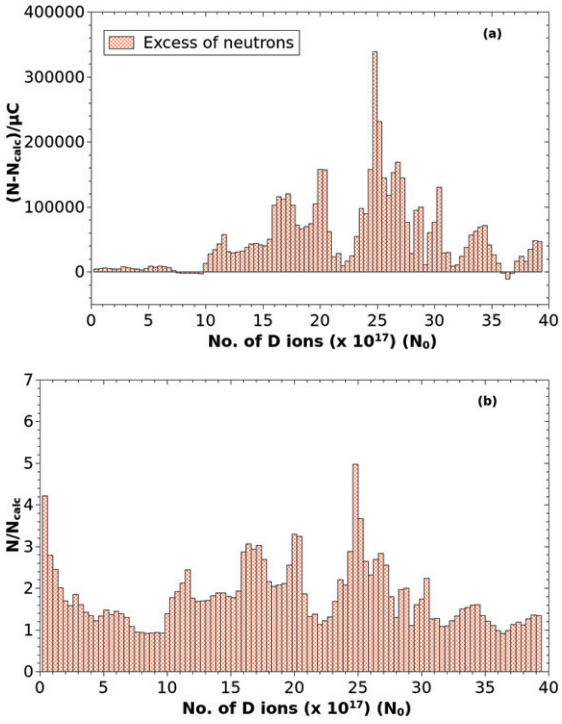

Fig. 8: (a) The excess (or deficiency) of neutrons with respect to the simulated value as a function of the number of implanted ions (N_0). (b) The ratio of measured neutrons to the simulated value as a function of the number of implanted ions.

GEANT4 for a given number of total implanted deuterium ions. For calculating the number of deuterium ions per cm^2, N_t, we have made the simplified assumption that the implanted deuterium ions are contained in a cylindrical volume with radius $\sim\sigma_{beam}$, the standard deviation of the beam profile which is taken as 2 mm and a length equal to the average range of 100 keV D^+ ions in Pd, $\sim$0.5 μm. The beam profile used for the simulation was a Gaussian with $\sigma = \sigma_{beam}$.

A typical 2D graph of the simulated ion distribution is shown in fig. 6(a) while the number of deuterium ions per cm^2 is shown as a function of depth in fig. 6(b) for a total number of D^+ ions of 2×10^{18}. The D^+ ion energy at the peak of the implantation profile is about 6–8 keV.

Figure 7 shows the experimental data of N/μC as a function of implanted ions along with the simulated result. As can be seen, the simulation explains the general trend. However, it fails to account for the oscillatory behaviour in the yield. It may be pointed out that at large D/Pd ratios, there could be strong diffusion [29] towards the target surface and this can cause a flattening of the initial ion distribution, thereby increasing the ion density at the surface layers. We have carried out the calculation in the extreme case of a flat distribution of ions extending up to the surface. As expected, this leads to an overall increase in the neutron yield all through the implantation curve and does not match with any of the observed data. In any case, the periodic fluctuations in the neutron yield observed in a certain range of D/Pd cannot be explained by the diffusion process alone.

The excess of neutrons observed over the simulated value (red solid curve in fig. 7) is plotted as a function of the total number of implanted D^+ ions (N_0) in fig. 8(a) while the ratio is shown in fig. 8(b). The excess of neutrons in a certain region is significantly large which might be ascribed to the strong matrix effect of the host material at large D/Pd ratios. This phenomenon needs further investigation using other host materials in order to examine the role of the host matrix in neutron production.

Summary. – In summary, the 2.45 MeV neutrons emitted in the $D + D$ fusion reaction occuring in a cooled palladium foil were measured as a function of the implanted D^+ ions. The N/μC as a function of the total implanted D^+ ions showed distinct oscillatory behaviour as opposed to the smooth trend seen in the calculations. This may be attributed to the complex microscopic dynamical effects arising from a combination of screening and diffusion in the metal lattice at high D/Pd ratios. More measurements are required in order to understand the present observations in detail by varying the parameters such as bombarding energy and host metal temperature.

* * *

The authors gratefully acknowledge many fruitful discussions with Dr. S. S. Kapoor and are very thankful for his keen interest in this work. They also acknowledge the effort of Dr. A. K. Gupta and the ECR team for the smooth operation of the machine and for providing stable beams throughout the experiment. Thanks are also due to Dr. Suresh C. Parida of PDD, BARC, for providing the high-purity deuterium gas and Mr. Rohan Turbhekar, Target Lab, TIFR, for providing the palladium foils.

REFERENCES

[1] Pizzone R. G. *et al.*, *Astrophys. J.*, **786** (2014) 112.
[2] Goncharov P. R., *At. Data Nucl. Data Tables*, **120** (2017) 121.

[3] Ragheb M. and Nour Eldin A., *Fissile and fusile breeding in the thorium fusion fission hybrid*, in *Proceedings of the 1st International Nuclear & Renewable Energy Conference (INREC), Amman, 2010*, pp. 1–9.
[4] Prados-Estevez F. M., Subashiev A. V., Nee H. H., *Nucl. Instrum. Methods Phys. Res. B*, **407** (2017) 67.
[5] Czerski K. *et al.*, *EPL*, **113** (2016) 22001.
[6] Cvetinovic A., Lipoglavsek M., Markelj S. and Vesic J., *Phys. Rev. C*, **92** (2015) 065801.
[7] Tsyganov E. N., Bavizhev M. D., Buryakov M. G., Dabagov S. B., Golovatyuk V. M., Lobastov S. P., *Nucl. Instrum. Methods. Phys. Res. B*, **355** (2015) 333.
[8] Bystritsky V. M. *et al.*, *Nucl. Instrum. Methods Phys. Res. A*, **764** (2014) 42.
[9] Jelena Gajevic *et al.*, *Eur. Phys. J. A*, **49** (2013) 70.
[10] Bystritsky V. M. *et al.*, *Nucl. Phys. A*, **889** (2012) 93.
[11] Kalman Peter and Keszthelyi Tamas, *Phys. Rev. C*, **79** (2009) 031602(R).
[12] Czerski K. *et al.*, *J. Phys. G: Nucl. Part. Phys.*, **35** (2008) 014012.
[13] Czerski K. *et al.*, *Europhys. Lett.*, **54** (2001) 449.
[14] Raiola F. *et al.*, *Eur. Phys. J. A*, **13** (2002) 377.
[15] Raiola F. *et al.*, *Phys. Lett. B*, **547** (2002) 193.
[16] Kasagi J. *et al.*, *J. Phys. Soc. Jpn.*, **71** (2002) 2281.
[17] Huke A., Czerski K., Heide P., Ruprecht G., Targosz N. and Zebrowski W., *Phys. Rev. C*, **78** (2008) 015803.
[18] Huke A., Czerski K., Heide P., *Nucl. Instrum. Methods Phys. Res. B*, **256** (2007) 599.
[19] Kasagi Jirohta, *Surf. Coatings Technol.*, **201** (2007) 8574.
[20] Huke A., Czerski K., Dorsch T., Biller A., Heide P. and Ruprecht G., *Eur. Phys. J. A*, **27** (2006) 187.
[21] Raiola F. *et al.*, *Eur. Phys. J. A*, **27** (2006) 79.
[22] Tumino A. *et al.*, *Astrophys. J.*, **785** (2014) 96.
[23] Raiola F. *et al.*, *J. Phys. G: Nucl. Part. Phys.*, **31** (2005) 1141.
[24] Fang Kaihong, Zou Jianxin, Yoshida Eiji, Wang Tieshan and Kasagi Jirohta, *EPL*, **109** (2015) 22002.
[25] Bystritsky V. M. *et al.*, *Phys. At. Nuclei*, **75** (2012) 913.
[26] Agostinelli S. *et al.*, *Nucl. Instrum. Methods Phys. Res. A*, **506** (2003) 250.
[27] Rout P. C. *et al.*, *JINST*, **13** (2018) P01027.
[28] Choudhury R. K., Thomas R. G., Mohanty A. K. and Kapoor S. S., *Nucl. Sci. Eng.*, **169** (2011) 334.
[29] Myers S. M., Richards P. M., Follstaedt D. M. and Schirber J. E., *Phys. Rev. B*, **43** (1991) 9503.